Energization and Start-up of Modular Three-stage Solid State Transformers

Mariam Saeed, Alberto Rodríguez, Manuel Arias, Fernando Briz
Department of Electrical Engineering
University of Oviedo
Gijon, Asturias, Spain
saeedmariam@uniovi.es

José María Cuartas
INAEL Electrical Systems
Toledo, Spain

Abstract — **Grid-connection and startup of solid state transformers (SST) based on modular topologies are studied in this work. A simple solution is implemented to feed the auxiliary electronics (i.e. sensors, control boards, drivers, etc.) of each SST module. It is based on feeding this circuitry from the DC links of the module using Auxiliary Power Supplies (APS). However, this structure leads to a problematic energization of the SST due to the threshold input voltage of the APS. Before the DC link capacitors are charged to this voltage threshold, the APSs are not functional and consequently SST energization and connection to the grid are performed without monitoring. Although startup in this situation is problematic, adequate procedure can prevent unwanted transients. In this paper, a step-by-step simple procedure is proposed for energizing a three-stage SST based on a Cascaded H-Bridge (CHB) modular topology. Simulation results as well as experimental tests are presented.**

Keywords— **Solid State Transformers, Cascaded H-Bridge, modular, multilevel, auxiliary power supplies, grid forming, grid feeding, start-up, energization, pre-charging.**

I. INTRODUCTION

Solid State Transformers (SST) are the replacement for conventional Line Frequency Transformers (LFT). They are recently gaining research attention due to their wide range of functionalities in comparison to the LFTs [1], [2]. This is due to the fact that these smart transformers are formed by power electronic converters functioning at a relatively high switching frequencies. This enable them to provide many advantages like DC low voltage (LV) ports, controlled bidirectional power flow, protections, fault ride-through, imbalances and harmonics compensation [3]. These are appealing features for applications like smart grids to efficiently integrate distributed resources and storage systems. SSTs also provide a relevantly higher power density, which is of special interest for applications where volume and weight are critical. Good examples are traction, offshore and subsea applications [4]-[6]. On the other hand, there is always the question of reliability and robustness of the SST in comparison to the LFT and it is obvious that, in this aspect, the LFT is superior. However, recent achievements in the field of semiconductor devices are opening a way to a possible change of this. The faster switching speeds and higher blocking voltages of semiconductor devices can allow a possible relevant enhancement to the SST reliability [7].

Various examples of different SST topologies are available in literature [7]-[13]. The differences are mainly the number of stages and the modularity [14]. Three-stage topologies are preferable as they provide more flexibility, simpler control and commutation as well as optimization of the full SST by dividing it into three separate stages.

Modularity is mainly advantageous for achieving redundancy pushing the SST a step forward towards reliability. The importance of selecting a modular design is directly related to the required voltage levels that the SST has to interface as well as the rated power transfer that it has to process [14]. Non-modular multilevel topologies can be employed for high voltage grid levels, however, it compromises the redundancy and fault tolerance of the SST.

One of the widely used SST topologies is the modular three-stage topology where one stage is a modular AC/DC converter to interface with the medium/high voltage (MV/HV) grid, the second is a DC/DC converter and finally a DC/AC conventional LV converter to connect to the LV grid. Many works in literature have studied this SST structure focusing on the different aspects of modelling, control techniques, efficiency improvements, protections and fault tolerance [5]-[16]. However, few ideas are presented related to the energization and the start-up of this specific SST structure. In literature, this topic is mostly discussed for non-modular topologies. Moreover, to the best of the authors' knowledge no experimental results have been provided dealing with the first stages of the SST connection to the grid, including issues like pre-charging DC links, energizing auxiliary electronics in each of the SST modules, dealing with the possibility of operating in grid forming or grid feeding at any of the SST ports, etc.

In [17], the SST has a three-stage non-modular structure, in which the AC/DC stage is a conventional rectifier, the DC/DC stage is a dual half-bridge (DHB) and the DC/AC stage is a conventional inverter. The authors provided results for a straight forward stage-by-stage energization technique which resulted in high inrush current measured at the High Frequency Transformer (HFT). A procedure for decreasing this inrush current was proposed in [18]. The main idea was basically synchronizing the charging of the rectifier and the DC/DC stage DC links to achieve almost the same voltage at the terminals of the HFT. In [19], the SST topology is a three-stage non-modular multilevel structure based on a 3-level NPC converter acting as the AC/DC converter. In order to reduce the transients at the instant of the SST connection to the MV grid, charging of the MV DC link (22 kV) from the LV port is proposed. Regarding supplying the auxiliary electronics, in [20], strategies for implementing an Auxiliary Power Supply (APS) for a modular three-stage SST and a process to start it up are discussed. The work focuses on the design and the validation of the proposed APS but no simulation or experimental results of the start-up procedure are provided.

What specially distinguish the energization and start-up of the modular three-stage SSTs from other SST structures is the isolation requirements. It not only requires isolation between its two ports but also between series stacked

modules/cells at the HV side AC/DC converter stage which can be several kV over the LV side reference [21], [22]. Another important fact for practical SST application is the possibility of starting-up the SST with both grids available or with just one of them (i.e. grid-forming at one port) independent of the start-up port. In other words, depending on the availability of the grid, the SST has to be able to start-up from the HV side or from the LV side without any compromise in the behavior.

Those previously mentioned two facts imposes challenges on feeding the SST auxiliary electronics (i.e. energizing the SST) and its consequent start-up.

This paper proposes an APS structure fitting the topology practical implementation constrains. A simple step-by-step procedure for energizing and starting up the SST is presented. The method is then detailed for all possible SST operation modes depending on the availability of the grid at each of its ports. Validation of the proposed ideas is achieved using simulation and experimental results applied to the full-scale prototype of one SST module.

II. SST TOPOLOGY AND OPERATION MODES

A. SST topology

The selected SST topology is a three-phase CHB-based modular three-stage topology. It is schematically shown in Fig. 1 [23]. The topology is composed of three converters. The first stage is an AC/DC converter acting as the SST front-end converter connecting it to the HVAC grid. This stage is implemented using a CHB converter, whose cells are composed of a full-bridge (FB) and a DC link capacitor. Second stage is a DC/DC converter acting as the intermediate stage with the function of maintaining a required isolation level between both SST ports as well as bidirectional power flow. This stage uses a Dual Active Bridge (DAB) converter. The outputs of all the DABs of the three phases are connected in parallel creating a LV and high current DC link. Third stage is a conventional high-power DC/AC inverter which uses a 3-phase 4-line (3P4L) topology. Table I shows the specification of the SST. The AC/DC converter and the DC/DC converter stages have a modular structure. Each cell of the CHB is connected to one DAB converter forming one module of the SST (see Fig. 2). Modules are identical and stacked. Each module must be able to handle all the isolation required between the two SST ports. This is achieved by the DAB high frequency transformer (HFT).

The control of the SST is implemented in a partial distributed structure [24]. Each SST module has an independent control unit, this is called the Slave unit. Slave units are responsible for measurement and control tasks within the module, an example is generating gate signals for the CHB full-bridge, measuring input/output currents and voltages and performing the DAB control. However, there is a Master control unit where the top level control is implemented, dealing with balancing control of the CHB, measurement of line voltages and currents, grid synchronization, etc. All Slave control units of one phase are communicated together and to the Master control unit using a ring communication protocol based on TosNet. Each unit represents a node in the ring. This communication structure simplifies and reduces the optical fiber count [24].

B. Selected APS structure

The selected APS structure is a local distributed structure where APSs are used to feed the SST module from its local DC link capacitors. One APS is used to feed the HV side of the module from the cell capacitor (C_{cell} in Fig. 2). Another APS feeds the LV side of the module from the LV DC link capacitor (C_{LV} in Fig. 2).
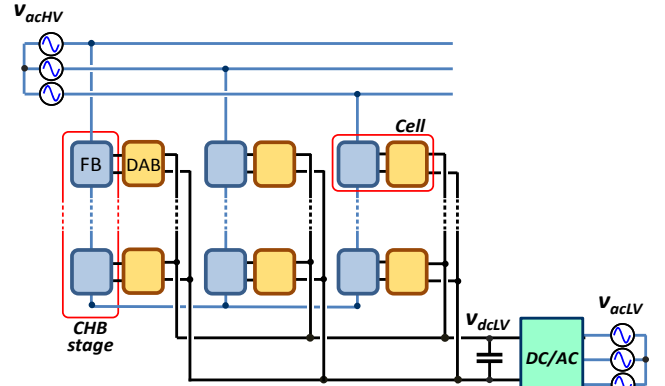

Fig. 1. : Selected modular-multilevel three-stage CHB based SST topology. AC grid filters at both ports are not shown.

TABLE I: SST SPECIFICATIONS

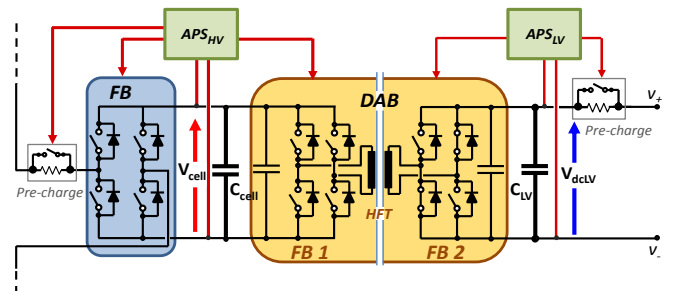| SST	
Rated power	105 kW
Number of cells	21 (7 per phase)
Rated power per module	5 kW
HV/LV grid voltage (L-L)	6 kV / 400 V
DAB	
Switching frequency	30 kHz
HFT isolation	24 kV
HFT transformation ratio	1:1
CHB	
V_{cell}	800 V
C_{cell}	600 µF(film)
LV DC/AC	
Rated power	105 kW
V_{dcLV}	800 V
C_{dcLV}	1500 µF (film)
APS	
Input voltage	800 V
Output voltage	24 V
Threshold (turn-on)	350 V

Fig. 2. : One module/cell of the SST composed of the CHB FB, DC link capacitor, the DAB FB1 and FB2, the HFT, the APSs and the HV/LV sides pre-charge circuits.

This structure allows the use of commercial APSs (for V_{cell} < 1500 V) [25], which are relatively cheap, and avoids the complexity of designing a high isolation power source. The fact of having a self-powered SST module preserves the redundancy of the SST, which intrinsic to its modular design, increasing the SST reliability.

Fig. 2 shows one module of the SST with the two APSs and their input and output connections.

C. SST operation modes

The SST can operate in many operation modes depending on the availability of the grid at each of its ports. If the grid is existing at a port, then this port is working in Grid-feeding. On the other hand, if the grid does not exist at a port, the port is working in Grid-forming and is required to create this grid. Since the three-stage CHB-based SST topology has two ports, three operation modes are possible. Each operation mode imposes a distinctive control structure for each of the converter stages of the SST. Each of these modes as well as the control function of each converter are explained in this section.

1) Both ports are operating in Grid-feeding (Fig. 3a):

In this case, both grids exist, and the grid-interfacing converters has to synchronize with the grid. The control of the HV side CHB converter is focused on balancing the cells capacitors (i.e. controlling V_{cell}) while the control of the LV DC/AC 3P4L converter is dedicated to maintaining the LV DC link capacitor at the target value (i.e. controlling V_{dcLV}). Finally, the DAB DC/DC converter control is responsible of controlling the power transfer between the two ports given that the voltage at both DC links is controlled at the required constant voltage.

2) LV port is operating in Grid-forming (Fig. 3b):

In this case, only the HV grid, V_{acHV}, is existing while the LV grid, V_{acLV}, is required to be formed by the SST. Similar to the previous case, the control task of the CHB converter is balancing the cells capacitors. However, the control of the LV DC link capacitor voltage, V_{dcLV}, has to be carried out by the DAB. It can no longer be performed through the DC/AC converter because its control will now be focused on creating/forming the LV grid. Since the DABs are all connected in parallel to the same C_{LV} DC link capacitor, the voltage control cannot be implemented in each DAB independently, instead, the outer voltage control loop is implemented in the Master control unit and the current reference is sent to all DABs.

3) HV port is operating in Grid-forming (Fig. 3c):

In this case, the LV grid, V_{acLV}, is existing while the HV grid, V_{acHV}, is formed by the SST. The CHB converter control is in charge of forming the HV grid while the balancing of the cell capacitor voltage is carried out by the DABs. Each DAB controls its V_{cell} independently. On the other hand, the LV side converter controls V_{dcLV}.

III. PROPOSED SST START-UP PROCEDURE

The aim of this section is, first, to clarify the challenges related to the energization and start-up of the selected SST topology based on the selected APS structure and second, to apply the proposed start-up technique step-by-step on all SST operation modes.
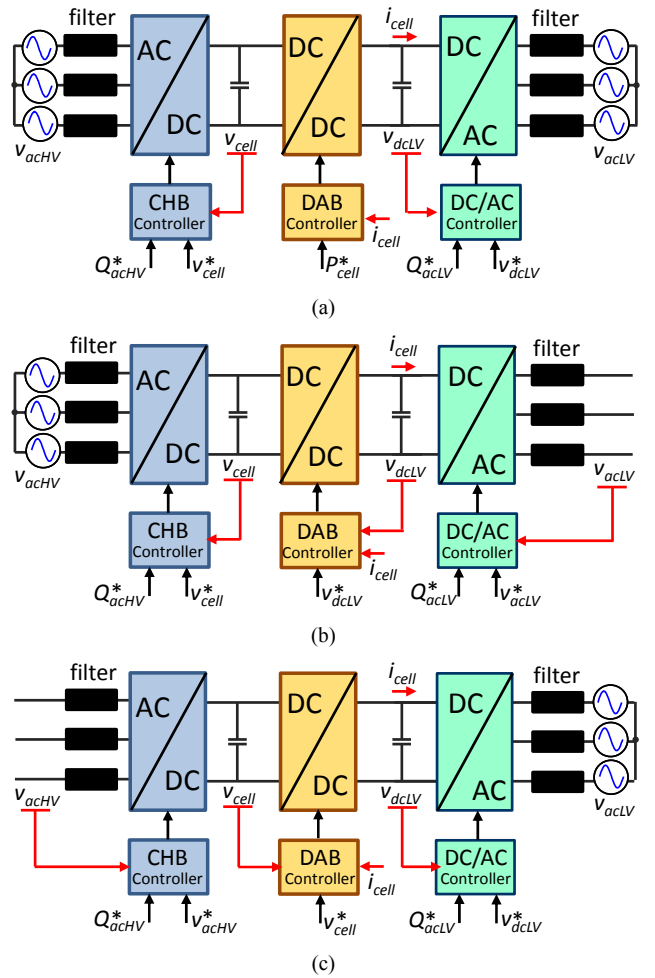
(a)

(b)

(c)

Fig. 3. : Operation modes of the SST. a) Both ports are operating in Grid-feeding, b) LV port is operating in Grid-forming, c) HV port is operating in Grid-forming. Existing grid is indicated using a sinusoidal voltage source. Control blocks for each converter stage are shown detailing the commands with (*) and the feedback signals in red. Active and reactive power are denoted as P and Q respectively.

A. SST Start-up challenges

The main challenge in this SST topology is the high isolation between HV and LV side grids, which is seen at the module level. While the proposed distributed APS structure provides the optimum solution for modular SST designs, providing simpler and more robust auxiliary circuitry energization technique, it implicates a more challenging start-up. The complication comes from two facts. The first one is that the APS has a threshold input voltage that should be achieved before it can feed any circuitry, implicating SST connection to the grid without any feedback or monetarization from the modules. The second one is that in a grid-forming situation, the forming port of the SST would be energized through the feeding port. This situation clearly leads to an uncontrolled energization, which may mean transient events such as inrush current and voltage drops/sags. These transients can lead to the possible breakdown of devices or drivers, saturation of HFT or switching off of the APSs.

B. Proposed start-up procedure

The three main characteristics of the proposed method for energizing and starting up the addressed SST topology

are the ability to mitigate undesired transients without any additional device or circuitry, validation for all operation modes and simplicity.

The basic idea of the proposed procedure is the synchronization of the energization/charging of the primary and secondary DC links, where the primary is the grid-feeding port and the secondary is the grid-forming port.

First, to charge the primary DC link from the rectifier connected to the grid, a pre-charge circuit is used to limit the inrush current. Two pre-charge circuits are essential at both ports of the SST (see Fig. 2) to be able to start-up in any operation mode (see Fig. 3). The value of the pre-charge resistors are selected based on the required time constant and the value of the DC link capacitor. The time constant is selected to be in the range of 600 ms. Resistor values are consequently calculated to be 1 kΩ for HV side and 450 Ω for LV side.

However, charging of secondary DC link is only possible after the energization of the corresponding APS (i.e. charging its feeding capacitor to the APS threshold voltage). Consequently, total synchronization (i.e. pre-charging both DC links at the same time) is not possible [18]. In this case, in order to avoid the inrush current resulting from the voltage difference applied on the transformer terminals, a soft starting technique is implemented as explained in detail in this section.

1) LV port operating in grid-feeding, HV port operating in grid-forming:

This operation mode takes place when the SST is supposed to establish the HVAC grid voltage while fed from the LVAC grid. Fig. 4 shows the detailed step-by-step proposed procedure for this particular operation mode. Since the grid is available at the LV side, it is obvious that the energization is done from this port. The blocks highlighted in blue are actions taking place at the LV side, while in red are those taking place at the HV side and in green are actions taking place simultaneously at both sides of the SST.

The procedure is also schematically shown in Fig. 5, where the LVAC grid rectified voltage, $V_{LVAC\ rectified}$ = 650 V (calculated based on the LVAC line voltage and the structure of the 3P4L converter) and T_r is the time constant which is defined by the pre-charge resistors and the value of C_{LV}. At step (3), when instantaneously enabling FB2 (DAB full-bridge of the LV side) to charge V_{cell}, an inrush current is prone to happen due to the instantaneous voltage applied to the terminals of the transformer. This inrush current would cause a voltage drop in V_{dcLV} introducing the possibility of switching Off APS_{LV} and losing power in the primary side. This issue is solved by soft-starting full-bridge FB2 at step (3). This is done by employing a low duty cycle [26]. At step (6), full control of the SST is achieved and it starts with its normal function (i.e. creating the HV grid and transferring power between both ports).

The theoretical method is validated using simulation results performed in Simulink Matlab® and applied to one module of the SST. The results are shown in Fig. 6.
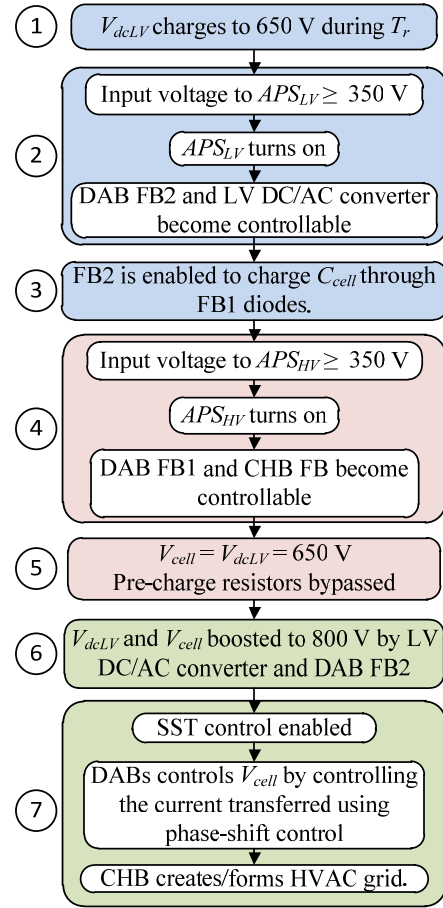

Fig. 4. : Block diagram showing step-by-step proposed procedure for SST start-up in the case of LV port operaing in grid-feeding and HV port operating in grid-forming.
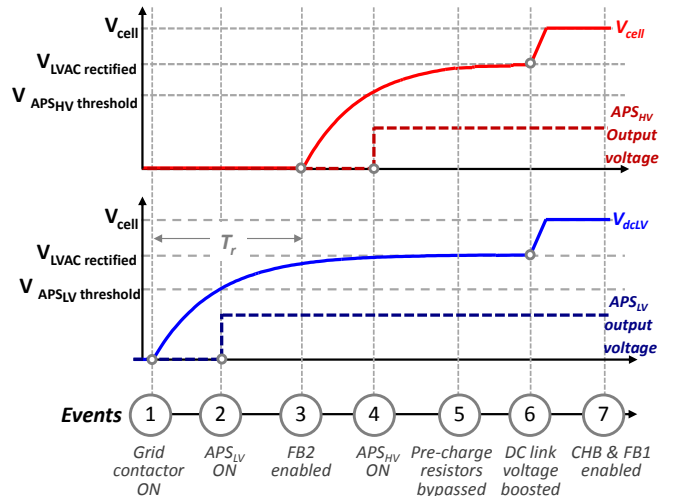

Fig. 5. : Schematic showing the events taking place during the proposed procedure for SST start-up in the case of LV port operaing in grid-feeding and HV port operating in grid-forming.

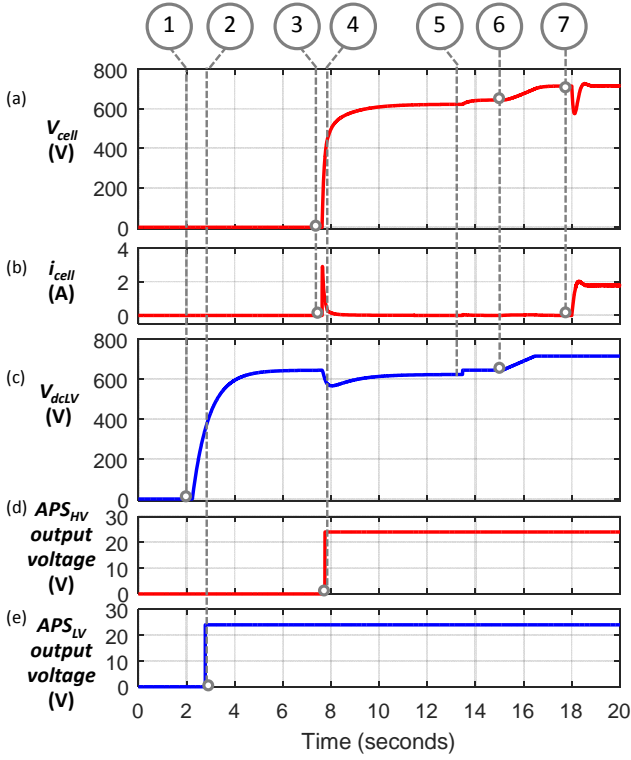Fig. 6. : Simulation results. Proposed procedure for SST start-up in the case of LV port operaing in grid-feeding and HV port operating in grid-forming, a) Cell voltage (V_{cell}), b) cell current (i_{cell}), c) LV DC link voltage (V_{dcLV}); d) APS_{HV} output voltage, e) APS_{LV} output voltage. Numbers at the top indicates events shown in Fig. 4 and Fig. 5.

2) HV port operating in grid-feeding, LV port operating in grid-forming:

This is the case when the SST is connected to the HVAC grid and is required to form the LVAC grid voltage. Fig. 7 shows the detailed step-by-step proposed energization and start-up procedure for this operation mode. Since the grid is available at the HV side, the energization is done from HV port. The blocks color coding is the same as the previous case.

The schematic of the start-up events is shown in Fig. 8, where the HVAC grid rectified voltage, $V_{HVAC\ rectified}$ = 606 V (calculated based on the HVAC line voltage and the structure of the CHB) and T_r is the time constant which is defined by the pre-charge resistors and the value of C_{cell}.

Similar to the previous operation mode, soft starting technique is implemented at step (3), in this case, when enabling FB1.

3) LV and HV ports operating in grid-feeding:

In this mode, the SST is connected to both the HVAC and the LVAC grids (i.e. both grid exist). Since the grid is available at both ports, the energization is done from both ports simultaneously. The start-up in this case is less problematic and previously discussed in literature [19]. Fig. 9 shows the detailed step-by-step start-up procedure. The blocks are only in green because events in HV and LV sides takes place simultaneously.

The start-up events are also schematically shown in Fig. 10. In this case each of C_{cell} and C_{LV} pre-charges to their corresponding grid rectified voltage (i.e. 606 V for C_{cell} and 650 V for C_{LV}).
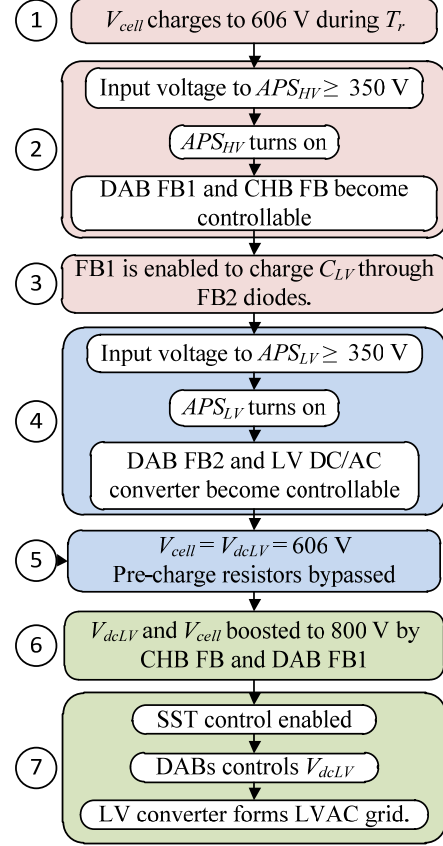

Fig. 7. : Block diagram showing step-by-step proposed procedure for SST start-up in the case of HV port operating in grid-feeding, LV port operating in grid-forming.
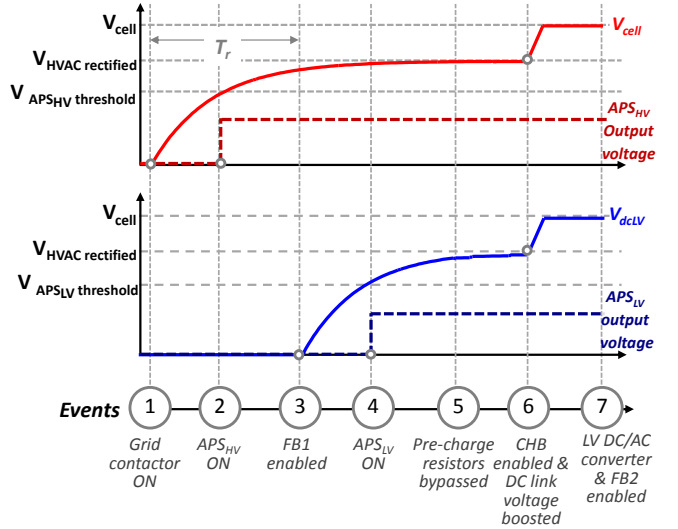

Fig. 8. : Schematic showing the events taking place during the proposed procedure for SST start-up in the case of HV port operating in grid-feeding, LV port operating in grid-forming.
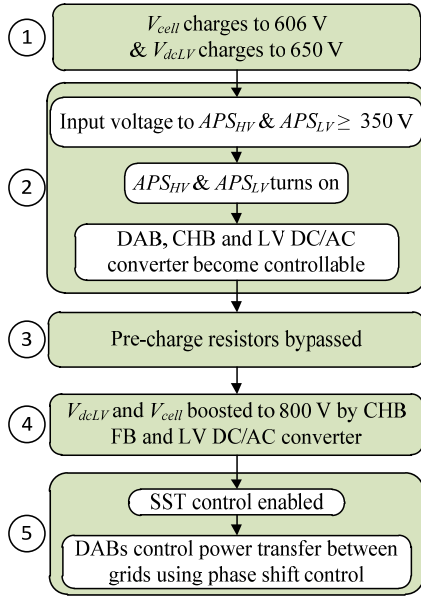
Fig. 9. : Block diagram showing step-by-step SST start-up procedure in the case of both LV and HV ports operating in grid-feeding.
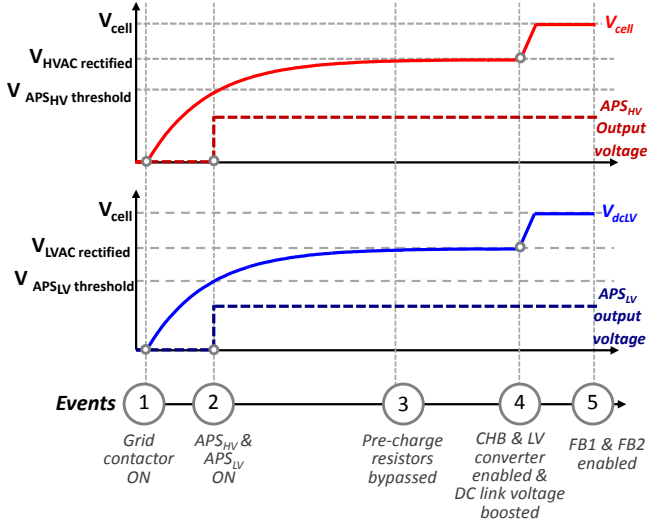

Fig. 10. : Schematic showing the events taking place during the SST start-up procedure in the case of both LV and HV ports operating in grid-feeding.
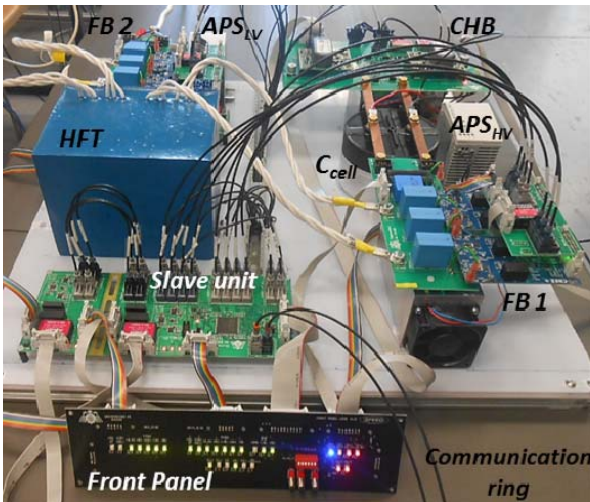

Fig. 11. : CHB-based SST module prototype (see Fig. 2).

IV. EXPERIMENTAL RESULTS

Fig. 11 shows the developed full-scale SST module. As shown in the corresponding schematic in Fig. 2, it is composed of the full bridge of the CHB, which is developed using 1.7-kV non-commercial Si IGBTs with a SiC anti-parallel diode from Infineon. The DAB bridges are developed using 1.2-kV commercial SiC MOSFETs from ROHM and two-channel commercial CREE driver boards. The control slave unit is designed based on a Xilinx Spartan 3E FPGA and including all AD converters and the required optical fibers for sending/receiving signals from all the module devices. The HFT is designed for 24-kV of galvanic isolation based on a UU-core and a separate winding structure [27]. The utilized APSs are commercial 60-W sources. The front panel board is designed to show the activity of all important components inside one module. Through the front panel it is possible to visualize any fault happening in the module as well as indicating the failing component.

Fig. 12 shows the experimental results when testing the proposed start-up procedure in the case of LV port operating in grid-feeding, and the HV port operating in grid-forming (Fig. 4 and Fig. 5). The test is carried out on the SST module (Fig. 11) at the target voltages. The results verifies the validity of the proposed start-up method.

Moreover, the obtained experimental waveforms (Fig. 12) are compared to the simulation waveforms (Fig. 6). The cell voltage in both cases is compared in Fig. 13. The noticeable agreement between the simulation and the experimental results validates the reliability of the developed simulation. This is a key point to the validation of the method on the full SST through simulation models.
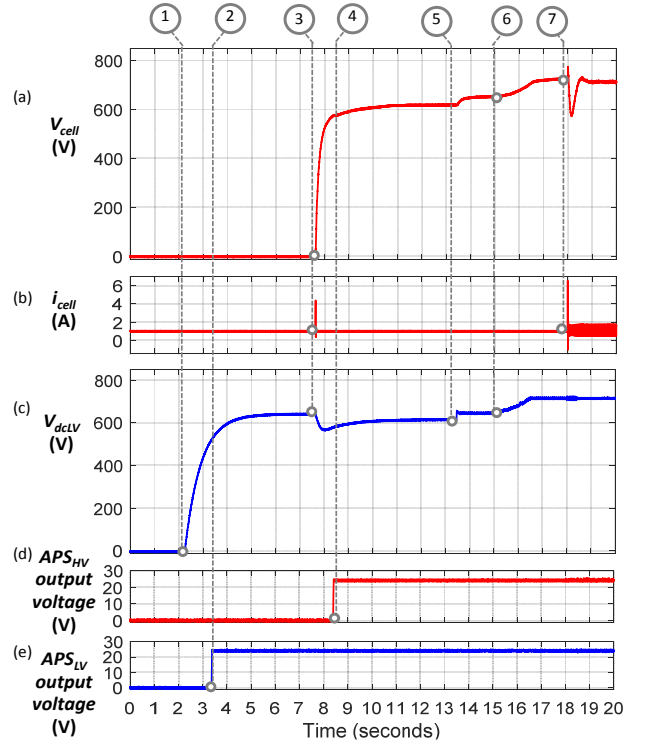

Fig. 12. : Experimental results. Proposed procedure for SST start-up in the case of LV port operaing in grid-feeding and HV port operating in grid-forming, a) Cell voltage (V_{cell}), b) cell current (i_{cell}), c) LV DC link voltage (V_{dcLV}), d) APS_{HV} output voltage, e) APS_{LV} output voltage. Numbers at the top indicates events shown in Fig. 4 and Fig. 5.
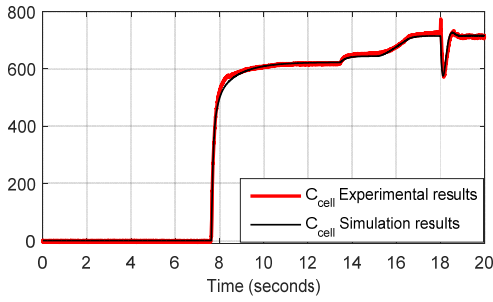
Fig. 13. : Comparison between the simulation and the experimentally measured cell voltage previously shown in Fig. 6 and Fig. 12.
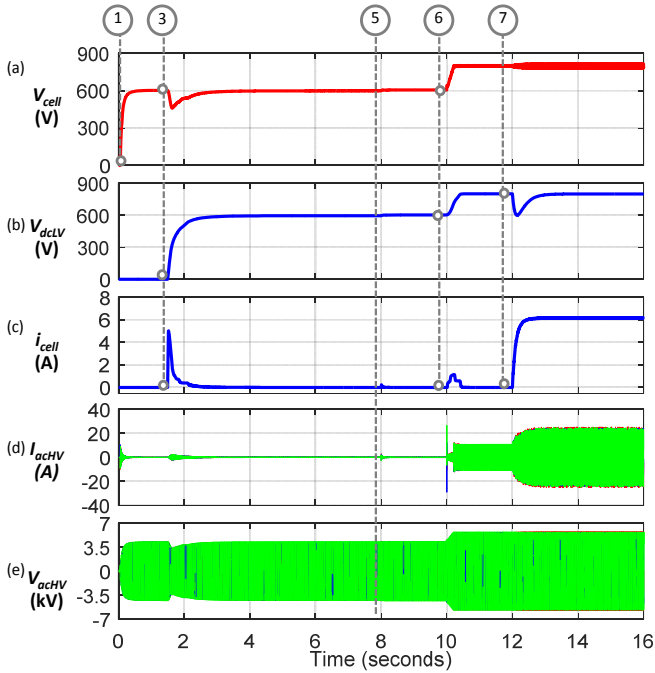

Fig. 14. : Simulation results. proposed procedure for SST start-up in the case of HV port operating in grid-feeding, LV port operating in grid-forming, a) Cell voltage (V_{cell}) of the first module in phase A b)) LV DC link voltage (V_{dcLV}), c) Cell current (i_{cell}), d) HV 3-phase line currents (I_{acHV}) and e) HV 3-phase line voltages (V_{acHV}). Numbers at the top indicates events shown in Fig. 7 and Fig. 8.

V. SIMULATION RESULTS FOR THE FULL SST

Since the SST is at a commissioning stage, experimental validation of the proposed method on the full SST is not possible. However, the proved reliability of the simulation model for one SST module opens the way to the development of a precise model for the full SST. This model allows the verification of the proposed method over the full SST. This simulation model is developed taking into consideration the details of the full structure, such as: grid filters, balancing control for the CHB cell capacitors, transients in line currents and voltages, etc.

Fig. 14 shows the simulation results for the case of the HV port operating in grid-feeding (procedure in Fig. 7). The obtained results proves the validity of the proposed method for starting up the SST with controlled transients.

VI. SUMMARY AND CONCLUSIONS

This work provides a discussion on the challenges and solutions to energize and start-up a three-stage CHB-based

modular multilevel SST. A distributed APS scheme is proposed to self-feed each SST module from its local LV DC links. This solution simplifies the design of the power source required to feed the auxiliary electronics, which may be complex due to the required high galvanic isolation between primary and secondary of one module. On the other hand, this APS structure provides a problematic energization in cases of grid-forming in one SST port. The fact that APSs are not operative till the DC links are pre-charged produces an uncontrolled initial start-up stage where transients are neither monitored nor controlled.

A simple step-by-step procedure to solve these challenges is presented in this work. The procedure is explained in details for all the SST operation modes. It is clearly seen that no additional circuitry nor complicated control is required.

REFERENCES

[1] J. W. van der Merwe and H. du T. Mouton, "The solid-state transformer concept: A new era in power distribution," *in AFRICON*, 2009, pp. 1–6.

[2] W. McMurray, "The thyristor electronic transformer: A power converter using a high-frequency link," *in IEEE Transaction on Ind. Gen. Appl.*, vol. IGA-7, no. 4, pp. 451–457, July 1971.

[3] J. E. Huber, and J. W. Kolar. "Solid-state transformers on the origins and Evolution of key concepts," in *IEEE Industrial Electronics Magazine,* vol.10, no.3, pp. 19-28, 2016.

[4] C. Gerster, "Smart transformers for traction: Status and challenges," presented at the *ECPE Workshop on Smart Transformers for Traction and Future Grid Applications*, Zurich, Switzerland, 2016.

[5] J. Taufiq, "Power electronics technologies for railway vehicles," in *Proc. Power Conversion Conf.,* Nagoya, Japan, 2007, pp. 1388–1393.

[6] J. Feng, W. Q. Chu, Z. Zhang and Z. Q. Zhu, "Power Electronic Transformer-Based Railway Traction Systems: Challenges and Opportunities," in *IEEE Journal of Emerging and Selected Topics in Power Electronics*, vol. 5, no. 3, pp. 1237-1253, Sept. 2017.

[7] A. Q. Huang, Q. Zhu, L. Wang and L. Zhang, "15 kV SiC MOSFET: An enabling technology for medium voltage solid state transformers," in *Transactions on Power Electronics and Applications*, vol. 2, no. 2, pp. 118-130, 2017.

[8] Xu She, A. Q. Huang, and R. Burgos, "Review of Solid-State Transformer Technologies and Their Application in Power Distribution Systems," in *IEEE Journal on Emerging and Selected Topics in Power Electronics*, vol. 1, no. 3, pp. 186–198, Sep. 2013.

[9] R. J. G. Montoya, A. Mallela and J. C. Balda, "An evaluation of selected solid-state transformer topologies for electric distribution systems," in *IEEE Applied Power Electronics Conference and Exposition (APEC)*, Charlotte, NC, 2015, pp. 1022-1029.

[10] S. Falcones, M. Xiaolin, and R. Ayyanar, "Topology comparison for solid state transformer implementation," in

Proc. IEEE Power and Energy Society General Meeting, 2010, pp. 1–8.

[11] H. Chen, A. Prasai and D. Divan, "Dyna-C: A Minimal Topology for Bidirectional Solid-State Transformers," in *IEEE Transactions on Power Electronics*, vol. 32, no. 2, pp. 995-1005, Feb. 2017.

[12] F. Blaabjerg, R. Teodorescu, M. Liserre, and A. V. Timbus, "Overview of control and grid synchronization for distributed power generation systems," in *IEEE Transactions on industrial electronics*, vol. 53, no. 5, pp. 1398–1409, 2006.

[13] B. Zhao, Q. Song, W. Liu, and Y. Sun, "Overview of dual-active-bridge isolated bidirectional dc–dc converter for high-frequency-link power conversion system," in *IEEE Transactions on Power Electronics*, vol. 29, no. 8, pp. 4091–4106, 2014.

[14] M. Andresen, L. F. Costa, G. Buticchi and M. Liserre, "Smart Transformer reliability and efficiency through modularity," in *IEEE 8th International Power Electronics and Motion Control Conference (IPEMC-ECCE Asia)*, Hefei, 2016, pp. 3241-3248.

[15] Q. Zhu, L. Wang, A. Huang, K. Booth and L. Zhang, "7.2 kV Single Stage Solid State Transformer Based on Current Fed Series Resonant Converter and 15 kV SiC MOSFETs," in *IEEE Transactions on Power Electronics*.

[16] S. Madichetty, B. Duggal, A. Borgaonkar and S. Mishra, "Modeling and design of solid state smart transformer for microgrid," in *IEEMA Engineer Infinite Conference (eTechNxT)*, New Delhi, 2018, pp. 1-6.

[17] K. Mainali, S. Madhusoodhanan, A. Tripathi, D. Patel and S. Bhattacharya, "Start-up scheme for solid state transformers connected to medium voltage grids," in *IEEE Applied Power Electronics Conference and Exposition (APEC),* Charlotte, NC, 2015, pp. 1014-1021.

[18] X. Liu, L. Liu, H. Li, K. Corzine and T. Guo, "Study on the start-up schemes for the three-stage solid state transformer applications," in *IEEE Energy Conversion Congress and Exposition (ECCE)*, Raleigh, NC, 2012, pp. 3528-3532.

[19] X. Liu, H. Li and Z. Wang, "A Start-Up Scheme for a Three-Stage Solid-State Transformer With Minimized Transformer Current Response," in *IEEE Transactions on Power Electronics,* vol. 27, no. 12, pp. 4832-4836, Dec. 2012.

[20] L. B. Kehler, A. M. Kaminski, J. R. Pinheiro, C. Rech, T. B. Marchesan and R. R. Emmel, "Auxiliary power supply for solid state transformers," in *IEEE International Conference on Electronics, Circuits and Systems (ICECS),* Monte Carlo, 2016, pp. 193-196.

[21] M. Saeed, J. M. Cuartas, A. Rodriguez, M. Arias and F. Briz, "Energization and start-up of CHB based modular three-stage Solid State Transformers," in *IEEE Transactions on Industry Applications*.

[22] D. Cottet et al., "Integration technologies for a medium voltage modular multi-level converter with hot swap capability," in *IEEE Energy Conversion Congress and Exposition (ECCE),* Montreal, QC, 2015, pp. 4502-4509.

[23] F. Briz, M. Lopez, A. Rodriguez and M. Arias, "Modular Power Electronic Transformers: Modular Multilevel Converter versus Cascaded H-Bridge Solutions," IEEE Industrial Electronics Magazine, vol. 10, no. 4, pp. 6-19, Dec. 2016.

[24] Lopez, M.; Rodriguez, A.; Blanco, E.; Saeed, M.; Martinez, A.; Briz, F., "Design and implementation of the control of an MMC-based solid state transformer," in *IEEE 13th International Conference on Industrial Informatics (INDIN)*, pp. 1583-1590, 22-24 July 2015.

[25] A. Rodriguez et al., "Auxiliary power supply based on a modular ISOP flyback configuration with very high input voltage," in *IEEE Energy Conversion Congress and Exposition (ECCE),* Milwaukee, WI, 2016, pp. 1-7.

[26] S. Inoue and H. Akagi, "A Bidirectional DC–DC Converter for an Energy Storage System with Galvanic Isolation," in *IEEE Transactions on Power Electronics*, vol. 22, no. 6, pp. 2299-2306, Nov.2007.

[27] M. Saeed, M. R. Rogina, M. López, A. Rodríguez, M. Arias and F. Briz, "Design and construction of a DAB using SiC MOSFETs with an isolation of 24 kV for PET applications," in *19th European Conference on Power Electronics and Applications (EPE'17 ECCE Europe)*, Warsaw, 2017, pp. P.1-P.10.